THE JOURNAL OF PHYSICAL CHEMISTRY B

Article

pubs.acs.org/JPCB

Effect of Side-Chain Length on Structural and Dynamic Properties of Ionic Liquids with Hydroxyl Cationic Tails

Kuo Wei,[†,‡] Li Deng,[†] Yanting Wang,[†,*] Zhong-Can Ou-Yang,[†] and Guodong Wang[‡]

[†]State Key Laboratory of Theoretical Physics, Institute of Theoretical Physics, Chinese Academy of Sciences, 55 East Zhongguancun Road, P.O. Box 2735, Beijing, 100190 China

[‡]College of Science, Northwest A&F University, 3 Taicheng Road, Yangling, Shaanxi, 712100 China

Supporting Information

ABSTRACT: The recent study has revealed that ionic liquids (ILs) with hydroxyl cationic tails are polar liquids without tightly aggregated nonpolar tail domains. Nevertheless, the influence of varying side-chain length on their microscopic structure and dynamics is still unclear. By performing all-atom molecular dynamics simulations for 1-(*n*-hydroxyalkyl)-3-methylimidazolium nitrate, where *n* varies from 2 to 12, we found that, with increasing side-chain length, both the nonpolar region and the flexibility of cationic tails increase. The larger nonpolar region pushes both the charged groups (heads and anions) and nonpolar groups (methylene groups on the side chains) to become more organized, while the increasing tail flexibility allows the hydroxyl terminals to retain a relatively uniform distribution. The increase of side-chain length does not apparently alter the polar nature of the ILs with hydroxyl tails, and has little effect on the total number of formed hydrogen bonds, but slows down the dynamics of ILs.

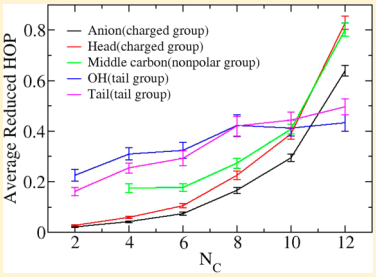

I. INTRODUCTION

Ionic liquids (ILs) have many promising applications in industry, including their wide applications as alternatives to hazardous solvents in organic synthesis[1] and as high-performance and versatile lubricants.[2−5] ILs also throw lights on various areas such as nanomaterials,[6] drug delivery,[7−9] embalming,[10] fuel cells,[11−14] and electrochemistry.[15−22] Therefore, a systematic understanding of their microscopic structures and dynamics is urgently needed. Many experimental and theoretical studies were devoted to investigate the behavior of ILs with amphiphilic properties.[23−29] Those studies made clear that, in ILs with alkyl side chains, tail groups can aggregate to form separate nonpolar tail domains due to the repulsion from polar groups (anions and cationic head groups). Recently, some researchers also extended their investigations to ILs with polar tails. Drummond et al.[30,31] found that the presence of hydroxyl groups on side chains leads to much less ordered liquids. Triolo et al.[32] discovered that the introduction of an ether side chain leads to the disappearance of the mesoscopic structural correlations observed in ILs with nonpolar side chains and the increase of the intermolecular interactions between alkyl groups. The study of hydroxylammonium-based ILs by both experiment and simulation revealed that those polar ILs are less fragile and strong interionic interactions exist due to the presence of hydrogen bonds.[33] The molecular dynamics (MD) simulations by Voth et al.[34] identified a glass-transition region and revealed a complex hydrogen-bond network in HEATN. By using MD simulations, Smith et al.[35] made a comparison of imidazolium-based ILs with alkyl and ether chains, respectively, and found that cation−anion and cation−cation interactions as well as nanoscale segregation of tails are weaker in ILs with ether chains. It was also reported that the hydroxyl-functionalization of an IL increases its viscosity, polarity, hydrophilicity, and hydrogen-bonding capability.[36−40] However, the molecular origin of the above observations for ILs with polar tails was unclear until the report of our previous work,[41] which suggested the microscopic mechanism that, by replacing one of the hydrogen atoms on the terminal methyl group by a hydroxyl group, the hydroxyl groups form a rich amount of hydrogen bonds with anions, cationic head groups, and other hydroxyl groups, which slows down the dynamics of ILs and changes the amphiphilic ILs to polar ILs without tightly aggregated nonpolar tail domains.

In order to reach the goal of providing the right IL by design to satisfy the requirement of a specific application, a theoretical understanding of the "tunability" of ILs, such as the influence of side-chain length on the structure and dynamics of ILs, is essential for their smart utilizations. The structural and dynamic changes of ILs with alkyl chains have been studied extensively. For instance, Huddleston et al.[42] found experimentally that, with increasing side-chain length, hydrophobicity and viscosity of nonpolar ILs increase, whereas density and surface tension decrease; the Ribeiro group[43] found that, by increasing the length of the side chain, the nearest anions are pushed away from the volume occupied by the flexible side chain; Wang et al.[44] revealed that the chain length has a significant effect on the structure of nonpolar ILs: when the side chain is sufficiently long, the structure of ILs changes from spatially heterogeneous

Received: October 14, 2013
Revised: March 9, 2014
Published: March 10, 2014

to liquid crystalline-like. Therefore, the influence of varying side-chain length on the microscopic structure and dynamics of ILs with polar tails is also of great interest. In this work, we perform all-atom MD simulations for 1-(*n*-hydroxyalkyl)-3-methylimidazolium nitrate (denoted as P_n with *n* varying from 2 to 12) ILs, whose cation molecular structure is shown in Figure 1, to study the influence of side-chain length on the

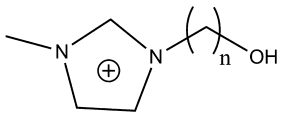

Figure 1. Molecular structure of the cations of 1-(*n*-hydroxyalkyl)-3-methylimidazolium nitrate, where *n* = 2, 4, 6, 8, 10, and 12.

structure and dynamics of ILs with hydroxyl tail groups. Our simulation results suggest that the structural heterogeneity and viscosity of ILs slightly increase with side-chain length, but the total number of formed hydrogen bonds has little changes and the increasing flexibility of side chains allows hydroxyl tails to retain a relatively uniform distribution.

II. SIMULATION METHODS

The P_n IL systems with *n* = 2, 4, 6, 8, 10, and 12 were simulated by the GROMACS MD simulation package[45] with the AMBER 94 force field,[46] exactly the same as the force field for P_8 reported in ref 41. The partial charges of the six cations are listed in Figure S1 in the Supporting Information. The initial configurations of all systems included 512 ion pairs evenly distributed in a very large cubic simulation box with the periodic boundary condition applied. A short energy minimization procedure was performed to achieve force convergence, followed by a simulated annealing procedure in the constant *NPT* ensemble with the initial temperature *T* = 2000 K down to 1500, 1000, 800, 600, and 400 K at a constant pressure *P* = 100 atm. At each temperature the MD simulation was performed for 1 ns. The last configuration at *T* = 400 K went through another *NPT* MD simulation with *P* = 1 atm for 1 ns to determine the average cubic simulation box size in equilibrium. The system was then fixed with this box size to perform another simulated annealing procedure in the constant *NVT* ensemble. The *NVT* annealing procedure started at *T* = 1000 K and then cooled down to 400 K with a temperature interval of 200 K. At each temperature the system was simulated for 1 ns. The last configuration at *T* = 400 K went through another MD simulation procedure to further equilibrate, whose simulation time varied for different systems: 20 ns for P_2 and P_4, 60 ns for P_6, P_8, and P_{10}, and 100 ns for P_{12}. The sampling was performed in the last 20 ns to obtain 2000 evenly distributed instantaneous configurations. The time step was 1 fs for all simulations.

To check the validity of the developed molecular models, the system densities were calculated according to our simulation data and compared to experimental values. The densities of the P_4, P_6, and P_8 systems are 1.2111, 1.1644, and 1.1178 g/cm^3, respectively, close to the experimentally measured 1.1283, 1.0892, and 1.0388 g/cm^3 at the temperature of 343.15 K and the pressure of about 100 kPa for the ILs with an alkyl terminal and the side-chain lengths of 4, 6, and 8, respectively.[47−49] The two sets of values are even closer if they are normalized by the molecular weights. Therefore, the molecular models we have developed for the P_n systems seem to be reasonably good at least for the qualitative studies reported in this work. Although it has been demonstrated that the polarizable models[50−53] for ILs are generally more accurate than nonpolarizable models (e.g., polarizable models usually provide faster dynamics closer to experiments), the polarizable models require much more simulation time. Since the current study is focused on qualitative properties rather than quantitative precisions, we have chosen to use the nonpolarizable models so that we can easily accumulate adequate statistical data.

III. RESULTS AND DISCUSSION

For convenience, throughout this paper we denote the center-of-mass (COM) position of the cationic headgroup as "head", the last carbon atom on the cationic tail as "tail", and the carbon atom in the middle of the side-chain as "middle carbon". In addition, "anion" refers to the position of the nitrogen atom in the nitrate anion, and "hydroxyl" refers to the position of the oxygen atom in the hydroxyl group.

1. Cationic Length. In order to quantify the flexibility of the cationic side chains, the distributions of the cationic lengths for different IL systems have been calculated and are plotted in Figure 2. Here the cationic length *d* is defined as the distance

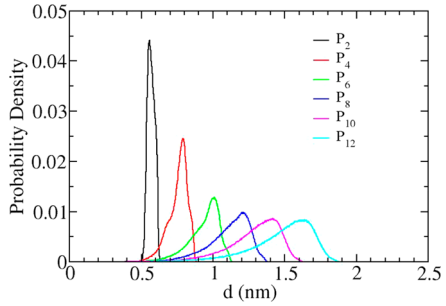

Figure 2. Distributions of the cationic length for different IL systems.

between the COM of the methyl group and the COM of the hydroxyl group. From Figure 2, we can see that, with increasing side-chain length, the most probable value of the cationic length increases, but the peak of the distribution decreases, and the distribution of *d* broadens, indicating that the flexibility of cationic side chains increases with chain length.

2. Spatial Heterogeneity. The reduced heterogeneity order parameter (HOP) defined in ref 54, whose value is around zero when the sites distribute almost uniformly, was used to quantify the spatial heterogeneity in the IL systems. The definitions of HOP and reduced HOP are briefly reviewed below.

The HOP of a given site of interest *i* is defined as

$$\hat{h}_i = \sum_{j=1}^{N_s} \exp(-r_{ij}^2/2\sigma^2) \quad (1)$$

where r_{ij} is the distance between sites *i* and *j*, corrected for periodic boundary conditions, and $\sigma = L/N_s^{1/3}$ with *L* the simulation box length and N_s the total number of sites in interest. The average HOP for a given configuration is the average value of HOPs for all sites in interest, which is defined as

$$\hat{h} = \frac{1}{N_s}\sum_{i=1}^{N_s} \hat{h}_i \quad (2)$$

dx.doi.org/10.1021/jp410168t | J. Phys. Chem. B 2014, 118, 3642−3649

The reduced HOP is defined as

$$h = \overset{\Lambda}{h} - \overset{\Lambda}{h}_0 \quad (3)$$

where $\overset{\Lambda}{h}_0$ is the HOP for the uniformly distributed configuration with the same number of sites, whose value can be found in ref 54. The theoretical relation between HOP and radial distribution function (RDF) is described in the Supporting Information of ref 55. It is apparent from the above definition that the reduced HOP takes a large value when the sites aggregate tightly and approaches zero when the sites distribute almost uniformly.

The instantaneous reduced HOPs for P_8 are plotted in Figure S2 in the Supporting Information. By averaging over all the sampled instantaneous configurations, the average reduced HOP values and their standard deviations for anions, head groups, hydroxyl groups, tail groups, and the middle carbon groups for all the studied IL systems have been calculated and are plotted in Figure 3. It can be seen that, with increasing side-chain length, the HOPs for all groups increase, indicating that all atoms in ILs are more organized and form sophisticated structures. On the other hand, the flexibility of cationic tails increases with chain length and larger amount of nonpolar methylene groups enhance the aggregation of nonpolar domains and push the charged groups (head groups and anions) to become more organized. Therefore, the HOPs of head groups, anions, and middle carbon groups increase quickly with side-chain length, but the greater flexibility allows the hydroxyl tails to retain their relatively uniform distribution and only slightly increase their degree of spatial heterogeneity. In contrast to the ILs with nonpolar tails whose spatial heterogeneity increase significantly with side-chain length,[54] the ILs with polar tails are dominated by the polar feature with very limited amphiphilic feature. Similar results were observed in the MD simulations of bicationic ILs studied by Li et al.,[56] where one cation with its associated anion can be regarded as a polar tail, resembling the hydroxyl group in our systems, despite the fact that the bicationic systems are more complex since the ions are much larger than the hydroxyls and not chemically bonded together.

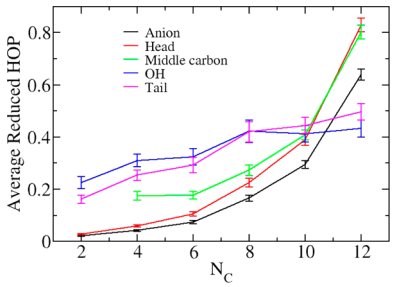

Figure 3. Average reduced HOPs for various atomic groups in the IL systems with different chain lengths. The error bars represent standard deviations.

3. Hydrogen Bonds. The number of hydrogen bonds in the IL systems was computed to see its change with side-chain length. A combination of A—H···B was determined as a hydrogen bond if the distance between atoms A and B is less than 0.35 nm and simultaneously the angle between A——H and A—B is less than 30°.[57] The average numbers of hydrogen bonds formed in all the polar IL systems are listed in Table S1 in the Supporting Information and plotted in Figure 4.

As listed in Table S1 in the Supporting Information, about 55% of hydrogen bonds in the polar IL systems are formed between anions and hydroxyl groups and about 38% of hydrogen bonds are formed between anions and head groups, which is attributed to the fact that the three oxygen atoms in each anion are all strong hydrogen-bond acceptors and the terminal hydroxyl groups and the three hydrogen atoms in each headgroup are hydrogen-bond donors.

From P_2 to P_8, the enlarged nonpolar region pushes the charged head groups and anions to become more organized, so the probability of forming hydrogen bonds between head

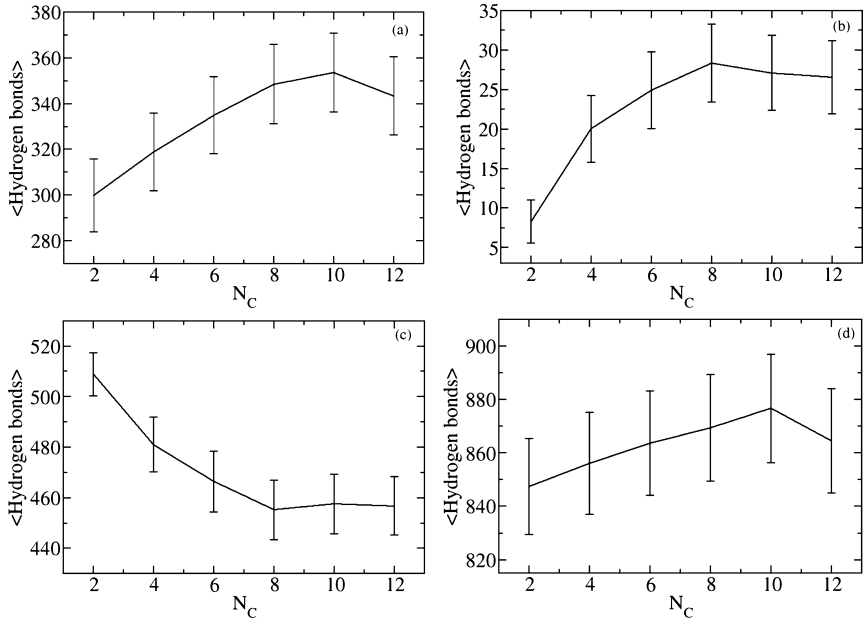

Figure 4. Average numbers of head-anion (a), OH−OH (b), anion−OH (c), and all (d) hydrogen bonds in different polar IL systems. The error bars represent standard deviations.

dx.doi.org/10.1021/jp410168t | J. Phys. Chem. B 2014, 118, 3642−3649

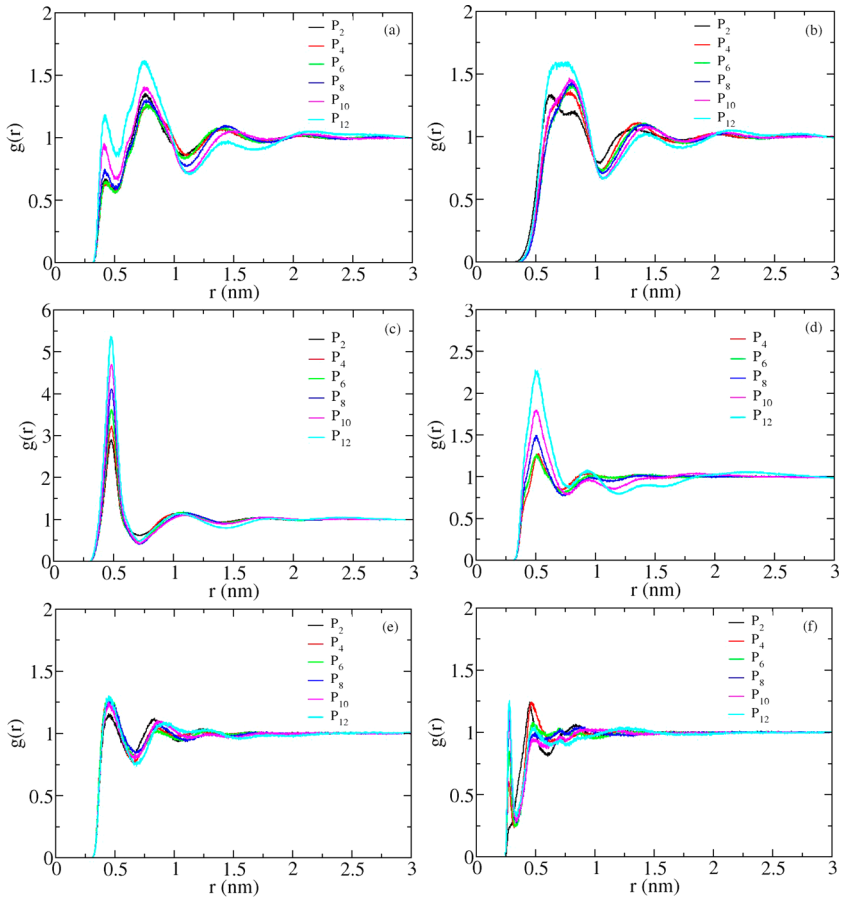

Figure 5. Radial distribution functions of head−head (a), anion−anion (b), head−anion (c), middle carbon−middle carbon (d), tail−tail (e), and OH−OH (f).

groups and anions increases with side-chain length (Figure 4a). At the same time, larger flexibility of the side chains allows hydroxyl groups to have more chance to become close and form hydrogen bonds. Therefore, from P_2 to P_8, the numbers of OH−OH hydrogen bonds increase monotonically (Figure 4b). Because of the increased occupation of anions and hydroxyls, the number of anion−OH hydrogen bonds decreases monotonically from P_2 to P_8 (Figure 4c). The numbers of all hydrogen bonds remain relatively unchanged from P_8 to P_{12}, probably due to the fact that all hydrogen-bond donor and acceptor sites are occupied. From P_2 to P_{12}, the total number of hydrogen bonds shows little change within the range of standard deviations (Figure 4d).

4. Radial Distribution Functions. The radial distribution functions (RDFs) for various groups have been calculated to characterize the structures and are plotted in Figure 5. Consistent with HOPs, from P_2 to P_{12}, the first peaks in the RDFs of head−head (Figure 5a), anion−anion (Figure 5b), head−anion (Figure 5c), and middle carbon-middle carbon (Figure 5d) increase quickly, but the tail−tail RDF (Figure 5e) does not change significantly, due to the fact that the increasing volume of the nonpolar carbon groups pushes the head groups and anions to be more structured, but the flexibility of the side chains allows the tail groups to retain their relatively uniform spatial distribution. The first peak at about 3 Å in the OH−OH RDF, corresponding to the number of hydrogen bonds formed between hydroxyl groups, increases its height from P_2 to P_8 and keeps almost unchanged from P_8 to P_{12} (Figure 5f), consistent with the change of number of hydrogen bonds between hydroxyl groups listed in Table S1.

In contrast, although the first peak at about 3 Å in the anion−OH RDF increases its height with chain length, the height of the second peak at about 5 Å decreases from P_2 to P_8 and keeps almost unchanged from P_8 to P_{12}. The integration of the two peak area, which roughly corresponds to the probability of forming hydrogen bonds, gives the same trend as the number of hydrogen bonds formed between anions and hydroxyls listed in Table S1. The change of tail-anion RDF is not monotonic since the tail groups are affected by both the hydroxyl groups and the nonpolar carbon groups.

5. Diffusion and Lifetimes. The mean square displacements (MSDs) of cations and anions in all systems were computed to investigate the influence of side-chain length on the dynamic properties of ILs. The diffusion coefficients were obtained by fitting the linear part of MSDs (MSDs for P_8 is given in Figure S3 in the Supporting Information as an example) according to the Einstein relation MSD = $6Dt$, where D is diffusion coefficient and t is time. As shown in Figure 6a, with increasing chain length, diffusion coefficients of both cations and anions become smaller, corresponding to slower dynamics.

In addition, we calculated the lifetime of ion pairs by continuous-time correlation function.[58] The lifetimes between head groups and anions and between hydroxyl groups and anions were calculated separately. Adopting the definition introduced in ref 58, the time correlation function $C(t)$ of ion pairs is defined as

dx.doi.org/10.1021/jp410168t | J. Phys. Chem. B 2014, 118, 3642−3649

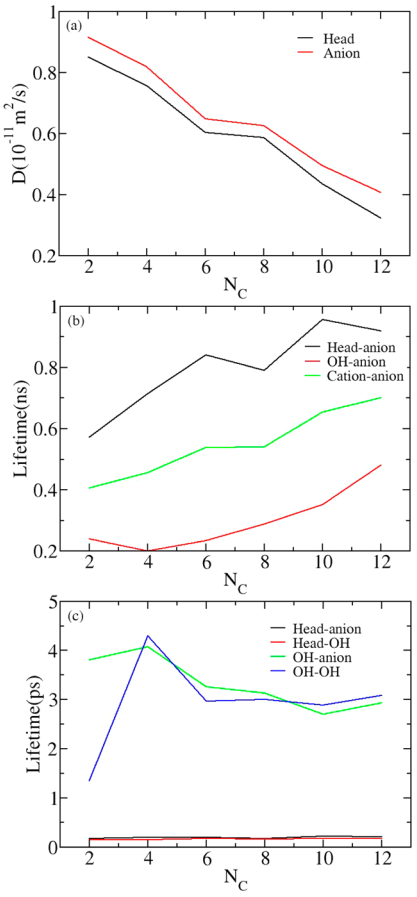

Figure 6. (a) Diffusion coefficients of head groups and anions. (b) Lifetimes of ion pairs. (c) Lifetimes of various hydrogen bonds.

$$C(t) = \frac{\langle p(0)P(t)\rangle}{\langle p(0)\rangle} \tag{4}$$

where $p(0) = 1$ if the distance between a cation and an anion is less than a certain threshold at the beginning, and $p(0) = 0$ otherwise. In contrast, $P(t) = 1$ holds only when the distance is less than the threshold all the time from the beginning until time t, and $P(t)$ is zero otherwise. The threshold value was taken to be 7 Å, roughly the radius of the first coordination shell. If the distance is less than the threshold, we regard the ion pair as intact, otherwise it is considered as broken. The angle brackets denote ensemble-average over all ion pairs and all starting times. From the definition, we can easily perceive that $C(t)$ describes the probability that an ion pair breaks at time t for the first time, given that it was intact at the starting time. We fitted the curves with three weighted exponentials:[58]

$$y = \alpha_1 \exp(-t/\tau_1) + \alpha_2 \exp(-t/\tau_2) + \alpha_3 \exp(-t/\tau_3) \tag{5}$$

where $\alpha_1 + \alpha_2 + \alpha_3 = 1$, and then we integrated the fitted function from zero to infinity to obtain the lifetime of ion pairs:

$$t_{life} = \alpha_1\tau_1 + \alpha_2\tau_2 + \alpha_3\tau_3 \tag{6}$$

The lifetimes of ion pairs are shown in Figure 6b, in which the lifetime of cation−anion is defined as the average value of head-anion and OH-anion (time correlation functions for P_8 are plotted in Figure S4 in the Supporting Information). The lifetime of head-anion is larger than that of OH-anion in all the IL systems, indicating that the correlation between head groups and anions is stronger than that between hydroxyl and anion. This can be easily understood by the fact that head groups carry net charges but hydroxyls only have dipole moments, so the electrostatic interactions between head groups and anions are stronger than the ones between hydroxyls and anions. The lifetime of cation−anion increases monotonically with chain length, indicating that interactions between cations and anions become stronger, which leads to slower dynamics of ILs.

It is interesting that both the diffusion coefficients (Figure 6a) and the lifetimes (Figure 6b) show discontinuities from P_6 to P_8. This might be understood as follows. When the side chain is short (P_2, P_4, and P_6), it is relatively rigid and the movement of the terminal hydroxyl group is closely correlated with the cationic head ring; when the side chain becomes longer (P_8, P_{10}, and P_{12}), it is more flexible and the terminal hydroxyl group moves more freely without much correlation with the cationic head ring. Therefore, the discontinuities of the diffusion coefficients and the lifetimes might correspond to the transition of the ILs from the "rigid side-chain phase" to the "flexible side-chain phase".

The lifetimes of hydrogen bonds between different groups are shown in Figure 6c (time correlation functions of hydrogen bonds for P_8 are plotted in Figure S5 in the Supporting Information). It is interesting that the hydrogen bonds between head groups and hydroxyls have similar lifetimes as those between head groups and anions. Similarly, the hydrogen bond lifetimes between hydroxyls and anions are close to those between hydroxyls and hydroxyls. However, the hydrogen bond lifetimes between anions and head groups are much shorter than those between anions and hydroxyls. This suggests that the polarity of the hydrogen bond donor plays the main role in determining the lifetime of a hydrogen bond. Since the protons on the hydroxyl tails are more polar than those on the cationic rings, the hydrogen bonds formed between hydroxyls and anions have longer lifetimes than those between head groups and anions, and the hydrogen bonds formed between hydroxyls and hydroxyls have longer lifetimes than those between head groups and hydroxyls. The hydrogen bonds between hydroxyls and hydroxyls in P_2 have a much shorter lifetime than those between hydroxyls and anions in P_2, which can be understood by considering that the cationic side chains in P_2 are very short and have little flexibility, so the hydrogen bonds formed between hydroxyls and hydroxyls are easy to break due to the motion and vibration of head groups and thus less stable than the hydrogen bonds between anions and hydroxyls. For P_4 to P_{12}, the above two types of hydrogen bonds have similar lifetimes, which slightly decrease with side-chain length, possibly due to the increasing flexibility of the side chains. For P_2 to P_{12}, the hydrogen bonds formed on head groups have almost exactly the same lifetimes, indicating that the side-chain length does not influence the lifetime of hydrogen bonds on head groups.

Comparing the results in parts b and c of Figure 6, one can see that head-anion has a longer lifetime than OH-anion, but the hydrogen bonds between head-anion have a shorter lifetime than those between OH-anion. This can be explained by the fact that one headgroup has three hydrogen-bond donors and one anion has three acceptors, so one head-anion pair can form up to nine hydrogen bonds and one hydroxyl can form up to three hydrogen bonds with one anion. Therefore, it is possible that the hydrogen bonds between a head-anion break and reform more frequently than those between an OH-anion without destroying the head-anion or OH-anion pair. This

dx.doi.org/10.1021/jp410168t | J. Phys. Chem. B 2014, 118, 3642−3649

indicates that the electrostatic interactions binding charged head groups and anions together dominate in the IL systems and the hydrogen bonds play a second role, consistent with the results reported in ref 59.

IV. CONCLUSIONS

In summary, we have performed all-atom molecular dynamics simulations for 1-(*n*-hydroxyalkyl)-3-methyl-imidazolium nitrate (identified as P_n), where *n* varies from 2 to 12, to investigate the changes of physical properties with respect to side-chain length. We found that, with increasing chain length, the nonpolar carbon groups on the side chains form larger nonpolar regions. Because the larger nonpolar regions push the head groups, middle carbon groups, and anions to be tighter and more organized, the degree of spatial heterogeneity of those groups apparently increases with chain length, but tail groups have much less change on the degree of spatial heterogeneity due to the increasing flexibility of side chains. Nevertheless, the increase of spatial heterogeneity is much milder than the IL systems with nonpolar tails.

From P_2 to P_8, with increasing chain length, the average number of hydrogen bonds between cations and anions increases because the polar groups come closer, and the hydroxyls also form more hydrogen bonds due to increasing flexibility of side chain. At the same time, anions and hydroxyls form fewer hydrogen bonds because more hydrogen bond sites are occupied. All numbers of hydrogen bonds do not change much from P_8 to P_{12}, possibly because all hydrogen bond sites are saturated. The total number of hydrogen bonds only has a slight change from P_2 to P_{12}, indicating that the slight increase of spatial heterogeneity with side-chain length does not alter the polar nature of the ILs with hydroxyl tails.

With increasing side-chain length, the correlation between anions and cations becomes stronger, which makes the dynamics of ILs slower. The time correlation between anions and head groups is much stronger than that between anions and hydroxyl groups, despite the fact that the lifetime of hydrogen bonds between anion-head is smaller than that between anion−OH, indicating that the electrostatic interactions dominate and hydrogen bonds only play a secondary role in ILs' dynamic properties, which is consistent with what has reported in ref 59.

■ ASSOCIATED CONTENT

Supporting Information

Partial charges of cations, number of hydrogen bonds, instantaneous HOPs, MSDs, time correlations for various groups, and time correlations of hydrogen bonds in the P_8 system. This material is available free of charge via the Internet at http://pubs.acs.org.

■ AUTHOR INFORMATION

Corresponding Author

*(Y.W.) E-mail: wangyt@itp.ac.cn. Telephone: +86 10-62648749.

Notes

The authors declare no competing financial interest.

■ ACKNOWLEDGMENTS

This work was supported by the National Basic Research Program of China (973 program, No. 2013CB932804), the National Natural Science Foundation of China (Nos. 11274319 and 11121403) and the Hundred Talent Program of the Chinese Academy of Sciences (CAS). The authors thank the Supercomputing Center in the Computer Network Information Center at the CAS for allocations of computer time.

■ REFERENCES

(1) Rogers, R. D.; Seddon, K. R. Ionic Liquids - Solvents of the Future? *Science* **2003**, *302*, 792−793.
(2) Ye, C.; Liu, W.; Chen, Y.; Yu, L. Room-Temperature Ionic Liquids: a Novel Versatile Lubricant. *Chem. Commun.* **2001**, 2244−2245.
(3) Liu, W.; Ye, C.; Gong, Q.; Wang, H.; Wang, P. Tribological Performance of Room-Temperature Ionic Liquids as Lubricant. *Tribol. Lett.* **2002**, *13*, 81−85.
(4) Qu, J.; Blau, P. J.; Dai, S.; Luo, H.; Meyer, H. M., III Ionic Liquids as Novel Lubricants and Additives for Diesel Engine Applications. *Tribol. Lett.* **2009**, *35*, 181−189.
(5) Bermúdez, M.-D.; Jiménez, A.-E.; Sanes, J.; Carrión, F.-J. Ionic Liquids as Advanced Lubricant Fluids. *Molecules* **2009**, *14*, 2888−2908.
(6) Antonietti, M.; Kuang, D.; Smarsly, B.; Zhou, Y. Ionic Liquids for the Convenient Synthesis of Functional Nanoparticles and Other Inorganic Nanostructures. *Angew. Chem., Int. Ed.* **2004**, *43*, 4988−4992.
(7) Hough, W. L.; Smiglak, M.; Rodríguez, H.; Swatloski, R. P.; Spear, S. K.; Daly, D. T.; Pernak, J.; Grisel, J. E.; Carliss, R. D.; Soutullo, M. D. The Third Evolution of Ionic Liquids: Active Pharmaceutical Ingredients. *New J. Chem.* **2007**, *31*, 1429−1436.
(8) Slowing, I. I.; Vivero-Escoto, J. L.; Wu, C.-W.; Lin, V. S.-Y. Mesoporous Silica Nanoparticles as Controlled Release Drug Delivery and Gene Transfection Carriers. *Adv. Drug. Deliv. Rev.* **2008**, *60*, 1278−1288.
(9) Viau, L.; Tourné-Péteilh, C.; Devoisselle, J.-M.; Vioux, A. Ionogels as Drug Delivery System: One-Step Sol−Gel Synthesis Using Imidazolium Ibuprofenate Ionic Liquid. *Chem. Commun.* **2010**, *46*, 228−230.
(10) Majewski, P.; Pernak, A.; Grzymisławski, M.; Iwanik, K.; Pernak, J. Ionic Liquids in Embalming and Tissue Preservation.: Can Traditional Formalin-Fixation be Replaced Safely? *Acta Histochem.* **2003**, *105*, 135−142.
(11) de Souza, R. F.; Padilha, J. C.; Gonçalves, R. S.; Dupont, J. Room Temperature Dialkylimidazolium Ionic Liquid-Based Fuel Cells. *Electrochem. Commun.* **2003**, *5*, 728−731.
(12) Susan, M. A.; Noda, A.; Mitsushima, S.; Watanabe, M. Brønsted Acid−Base Ionic Liquids and Their Use as New Materials for Anhydrous Proton Conductors. *Chem. Commun.* **2003**, 938−939.
(13) Lee, S.-Y.; Ogawa, A.; Kanno, M.; Nakamoto, H.; Yasuda, T.; Watanabe, M. Nonhumidified Intermediate Temperature Fuel Cells Using Protic Ionic Liquids. *J. Am. Chem. Soc.* **2010**, *132*, 9764−9773.
(14) Nakamoto, H.; Watanabe, M. Brønsted Acid−Base Ionic Liquids for Fuel Cell Electrolytes. *Chem. Commun.* **2007**, 2539−2541.
(15) Ohno, H. *Electrochemical Aspects of Ionic Liquids*, 2nd ed.; John Wiley & Sons: Hoboken, NJ, 2011.
(16) Wilkes, J. S.; Levisky, J. A.; Wilson, R. A.; Hussey, C. L. Dialkylimidazolium Chloroaluminate Melts: a New Class of Room-Temperature Ionic Liquids for Electrochemistry, Spectroscopy and Synthesis. *Inorg. Chem.* **1982**, *21*, 1263−1264.
(17) Lu, W.; Fadeev, A. G.; Qi, B.; Smela, E.; Mattes, B. R.; Ding, J.; Spinks, G. M.; Mazurkiewicz, J.; Zhou, D.; Wallace, G. G. Use of Ionic Liquids for π-Conjugated Polymer Electrochemical Devices. *Science* **2002**, *297*, 983−987.
(18) Buzzeo, M. C.; Evans, R. G.; Compton, R. G. Non-Haloaluminate Room-Temperature Ionic Liquids in Electrochemistry—a Review. *ChemPhysChem* **2004**, *5*, 1106−1120.
(19) Galiński, M.; Lewandowski, A.; Stępniak, I. Ionic Liquids as Electrolytes. *Electrochim. Acta* **2006**, *51*, 5567−5580.
(20) Sato, T.; Masuda, G.; Takagi, K. Electrochemical Properties of Novel Ionic Liquids for Electric Double Layer Capacitor Applications. *Electrochim. Acta* **2004**, *49*, 3603−3611.

(21) Hapiot, P.; Lagrost, C. Electrochemical Reactivity in Room-Temperature Ionic Liquids. *Chem. Rev.* **2008**, *108*, 2238−2264.
(22) Silvester, D. S.; Compton, R. G. Electrochemistry in Room Temperature Ionic Liquids: a Review and Some Possible Applications. *Z. Phys. Chem.* **2006**, *220*, 1247−1274.
(23) Canongia Lopes, J. N.; Pádua, A. A. Nanostructural Organization in Ionic Liquids. *J. Phys. Chem. B* **2006**, *110*, 3330−3335.
(24) Russina, O.; Triolo, A. New Experimental Evidence Supporting the Mesoscopic Segregation Model in Room Temperature Ionic Liquids. *Faraday Discuss.* **2012**, *154*, 97.
(25) Bhargava, B. L.; Devane, R.; Klein, M. L.; Balasubramanian, S. Nanoscale Organization in Room Temperature Ionic Liquids: a Coarse Grained Molecular Dynamics Simulation Study. *Soft Matter* **2007**, *3*, 1395.
(26) Wang, Y.; Voth, G. A. Tail Aggregation and Domain Diffusion in Ionic Liquids. *J. Phys. Chem. B* **2006**, *110*, 18601−18608.
(27) Wang, Y.; Voth, G. A. Unique Spatial Heterogeneity in Ionic Liquids. *J. Am. Chem. Soc.* **2005**, *127*, 12192−12193.
(28) Habasaki, J.; Ngai, K. L. Heterogeneous Dynamics of Ionic Liquids from Molecular Dynamics Simulations. *J. Chem. Phys.* **2008**, *129*, 194501.
(29) Schroder, C.; Rudas, T.; Neumayr, G.; Gansterer, W.; Steinhauser, O. Impact of Anisotropy on the Structure and Dynamics of Ionic Liquids: a Computational Study of 1-Butyl-3-Methyl-Imidazolium Trifluoroacetate. *J. Chem. Phys.* **2007**, *127*, 044505.
(30) Greaves, T. L.; Kennedy, D. F.; Mudie, S. T.; Drummond, C. J. Diversity Observed in the Nanostructure of Protic Ionic Liquids. *J. Phys. Chem. B* **2010**, *114*, 10022−10031.
(31) Pensado, A. S.; Gomes, M. F. C.; Lopes, J. N. C.; Malfreyt, P.; Pádua, A. A. Effect of Alkyl Chain Length and Hydroxyl Group Functionalization on the Surface Properties of Imidazolium Ionic Liquids. *Phys. Chem. Chem. Phys.* **2011**, *13*, 13518−13526.
(32) Triolo, A.; Russina, O.; Caminiti, R.; Shirota, H.; Lee, H. Y.; Santos, C. S.; Murthy, N. S.; Castner, J. E. W. Comparing Intermediate Range Order for Alkyl- vs. Ether-Substituted Cations in Ionic Liquids. *Chem. Commun.* **2012**, *48*, 4959−4961.
(33) Aparicio, S.; Atilhan, M.; Khraisheh, M.; Alcalde, R. Study on Hydroxylammonium-Based Ionic Liquids. I. Characterization. *J. Phys. Chem. B* **2011**, *115*, 12473−12486.
(34) Jiang, W.; Yan, T.; Wang, Y.; Voth, G. A. Molecular Dynamics Simulation of the Energetic Room-Temperature Ionic Liquid, 1-Hydroxyethyl-4-Amino-1,2,4-Triazolium Nitrate (HEATN). *J. Phys. Chem. B* **2008**, *112*, 3121−3131.
(35) Smith, G. D.; Borodin, O.; Li, L.; Kim, H.; Liu, Q.; Bara, J. E.; Gin, D. L.; Nobel, R. A Comparison of Ether- and Alkyl-Derivatized Imidazolium-Based Room-Temperature Ionic Liquids: a Molecular Dynamics Simulation Study. *Phys. Chem. Chem. Phys.* **2008**, *10*, 6301−6312.
(36) Tang, S.; Baker, G. A.; Zhao, H. Ether- and Alcohol-Functionalized Task-Specific Ionic Liquids: Attractive Properties and Applications. *Chem. Soc. Rev.* **2012**, *41*, 4030−4066.
(37) Dzyuba, S. V.; Bartsch, R. A. Expanding the Polarity Range of Ionic Liquids. *Tetrahedron Lett.* **2002**, *43*, 4657−4659.
(38) Ab Rani, M.; Brant, A.; Crowhurst, L.; Dolan, A.; Lui, M.; Hassan, N.; Hallett, J.; Hunt, P.; Niedermeyer, H.; Perez-Arlandis, J. Understanding the Polarity of Ionic Liquids. *Phys. Chem. Chem. Phys.* **2011**, *13*, 16831−16840.
(39) Holbrey, J. D.; Turner, M. B.; Reichert, W. M.; Rogers, R. D. New Ionic Liquids Containing an Appended Hydroxyl Functionality from the Atom-Efficient, One-Pot Reaction of 1-Methylimidazole and Acid with Propylene Oxide. *Green Chem.* **2003**, *5*, 731−736.
(40) Schrekker, H. S.; Stracke, M. P.; Schrekker, C. M.; Dupont, J. Ether-Functionalized Imidazolium Hexafluorophosphate Ionic Liquids for Improved Water Miscibilities. *Ind. Eng. Chem. Res.* **2007**, *46*, 7389−7392.
(41) Deng, L.; Shi, R.; Wang, Y.; Ou-Yang, Z.-C. Hydrogen-Bond Rich Ionic Liquids with Hydroxyl Cationic Tails. *Chem. Phys. Lett.* **2013**, *560*, 32−36.
(42) Huddleston, J. G.; Visser, A. E.; Reichert, W. M.; Willauer, H. D.; Broker, G. A.; Rogers, R. D. Characterization and Comparison of Hydrophilic and Hydrophobic Room Temperature Ionic Liquids Incorporating the Imidazolium Cation. *Green Chem.* **2001**, *3*, 156−164.
(43) Urahata, S. M.; Ribeiro, M. C. Structure of Ionic Liquids of 1-Alkyl-3-Methylimidazolium Cations: a Systematic Computer Simulation Study. *J. Chem. Phys.* **2004**, *120*, 1855−63.
(44) Ji, Y.; Shi, R.; Wang, Y.; Saielli, G. Effect of the Chain Length on the Structure of Ionic Liquids: from Spatial Heterogeneity to Ionic Liquid Crystals. *J. Phys. Chem. B* **2013**, *117*, 1104−9.
(45) Hess, B.; Kutzner, C.; Van Der Spoel, D.; Lindahl, E. GROMACS 4: Algorithms for Highly Efficient, Load-Balanced, and Scalable Molecular Simulation. *J. Chem. Theory Comput.* **2008**, *4*, 435−447.
(46) Cornell, W. D.; Cieplak, P.; Bayly, C. I.; Gould, I. R.; Merz, K. M.; Ferguson, D. M.; Spellmeyer, D. C.; Fox, T.; Caldwell, J. W.; Kollman, P. A. A Second Generation Force Field for the Simulation of Proteins, Nucleic Acids, and Organic Molecules. *J. Am. Chem. Soc.* **1995**, *117*, 5179−5197.
(47) Mokhtarani, B.; Sharifi, A.; Mortaheb, H. R.; Mirzaei, M.; Mafi, M.; Sadeghian, F. Density and Viscosity of 1-Butyl-3-Methylimidazolium Nitrate with Ethanol, 1-Propanol, or 1-Butanol at Several Temperatures. *J. Chem. Thermodyn.* **2009**, *41*, 1432−1438.
(48) Seddon, K. R.; Stark, A.; Torres, M.-J. Viscosity and Density of 1-Alkyl-3-Methylimidazolium Ionic Liquids. In *Clean Solvents*; Abraham, M., Moens, L., Eds.; ACS Symposium Series 819; American Chemical Society: Washington, DC, 2002; pp 34−49.
(49) Mokhtarani, B.; Sharifi, A.; Mortaheb, H. R.; Mirzaei, M.; Mafi, M.; Sadeghian, F. Densities and Viscosities of Pure 1-Methyl-3-Octylimidazolium Nitrate and its Binary Mixtures with Alcohols at Several Temperatures. *J. Chem. Eng. Data* **2010**, *55*, 3901−3908.
(50) Bedrov, D.; Borodin, O. Thermodynamic, Dynamic, and Structural Properties of Ionic Liquids Comprised of 1-Butyl-3-Methylimidazolium Cation and Nitrate, Azide, or Dicyanamide Anions. *J. Phys. Chem. B* **2010**, *114*, 12802−12810.
(51) Bedrov, D.; Borodin, O.; Li, Z.; Smith, G. D. Influence of Polarization on Structural, Thermodynamic, and Dynamic Properties of Ionic Liquids Obtained from Molecular Dynamics Simulations. *J. Phys. Chem. B* **2010**, *114*, 4984−4997.
(52) Yan, T.; Wang, Y.; Knox, C. On the Structure of Ionic Liquids: Comparisons between Electronically Polarizable and Nonpolarizable Models I. *J. Phys. Chem. B* **2010**, *114*, 6905−6921.
(53) Yan, T.; Wang, Y.; Knox, C. On the Dynamics of Ionic Liquids: Comparisons between Electronically Polarizable and Nonpolarizable Models II. *J. Phys. Chem. B* **2010**, *114*, 6886−6904.
(54) Wang, Y.; Jiang, W.; Voth, G. A. Spatial Heterogeneity in Ionic Liquids. In *Ionic Liquids IV: Not Just Solvents Anymore*; Brennecke, J. F., Rogers, R. D., Seddon, K. R., Eds.; ACS Symposium Series 975; American Chemical Society: Washington, DC, 2007; pp 272−307.
(55) Deng, L.; Wang, Y.; Ou-Yang, Z.-C. Concentration and Temperature Dependences of Polyglutamine Aggregation by Multi-scale Coarse-Graining Molecular Dynamics Simulations. *J. Phys. Chem. B* **2012**, *116*, 10135−10144.
(56) Li, S.; Feng, G.; Bañuelos, J. L.; Rother, G.; Fulvio, P. F.; Dai, S.; Cummings, P. T. Distinctive Nanoscale Organization of Dicationic versus Monocationic Ionic Liquids. *J. Phys. Chem. C* **2013**, *117*, 18251−18257.
(57) Luzar, A.; Chandler, D. Structure and Hydrogen Bond Dynamics of Water−Dimethyl Sulfoxide Mixtures by Computer Simulations. *J. Chem. Phys.* **1993**, *98*, 8160.
(58) Zhao, W.; Leroy, F.; Heggen, B.; Zahn, S.; Kirchner, B.; Balasubramanian, S.; Müller-Plathe, F. Are There Stable Ion-Pairs in Room-Temperature Ionic Liquids? Molecular Dynamics Simulations of 1-N-Butyl-3-Methylimidazolium Hexafluorophosphate. *J. Am. Chem. Soc.* **2009**, *131*, 15825−15833.
(59) Kohagen, M.; Brehm, M.; Lingscheid, Y.; Giernoth, R.; Sangoro, J.; Kremer, F.; Naumov, S.; Iacob, C.; Karger, J.; Valiullin, R.; Kirchner, B. How Hydrogen Bonds Influence the Mobility of Imidazolium-Based

Ionic Liquids. a Combined Theoretical and Experimental Study of 1-N-Butyl-3-Methylimidazolium Bromide. *J. Phys. Chem. B* **2011**, *115*, 15280−8.